IEEE Photonics Journal
An IEEE Photonics Society Publication

Open Access

Research on Biological Detection Based on Reflected Light Images of a Porous Silicon Bragg Mirror

Volume 13, Number 2, April 2021

Shuangshuang Zhang
Miao Sun
Jianfeng Yang
Zhenhong Jia
Xiaoyi Lv
Xiaohui Huang

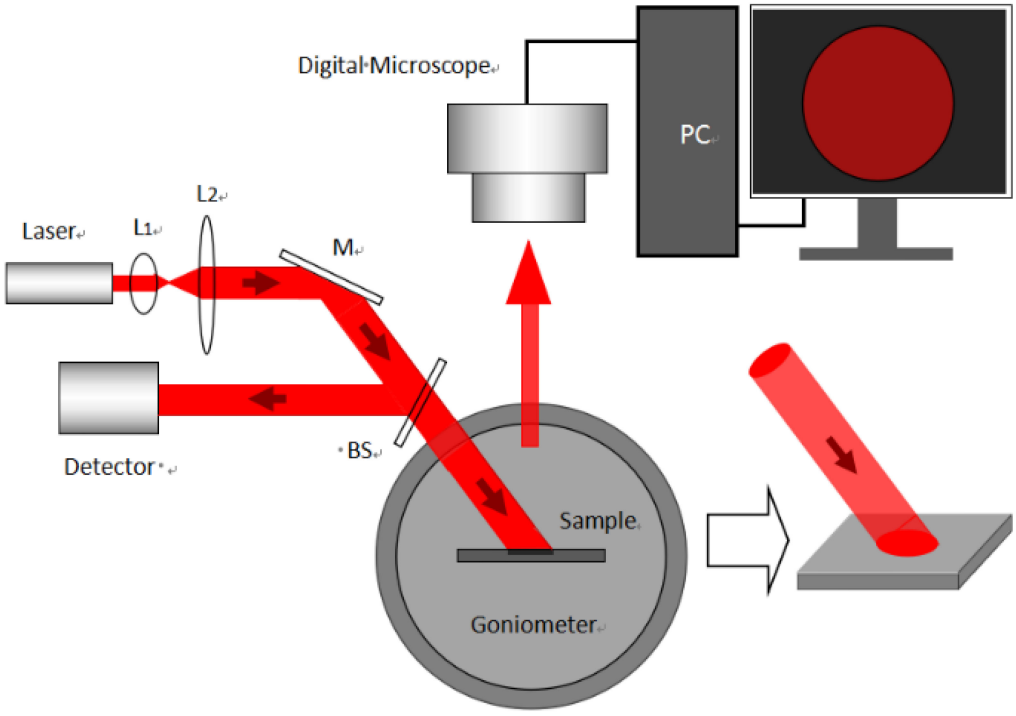

DOI: 10.1109/JPHOT.2021.3059684

Research on Biological Detection Based on Reflected Light Images of a Porous Silicon Bragg Mirror

Shuangshuang Zhang,[1] Miao Sun,[1] Jianfeng Yang,[1] Zhenhong Jia,[2,3] Xiaoyi Lv,[2,3] and Xiaohui Huang[2,3]

[1]School of Physical Science and Technology, Xinjiang University, Urumqi 830046, China
[2]School of Information Science and Engineering, Xinjiang University, Urumqi 830046, China
[3]The Key Laboratory of Signal Detection and Processing, Xinjiang Uygur Autonomous Region, Xinjiang University, Urumqi 830046, China

DOI:10.1109/JPHOT.2021.3059684

Manuscript received February 2, 2021; accepted February 12, 2021. Date of publication February 16, 2021; date of current version March 9, 2021. This work was supported in part by the National Key R&D Program of China under Grant 2019YFC1606100 and in part by the National Natural Science Foundation of China under Grant 61665012. Corresponding author: Zhenhong Jia (e-mail: jzhh@xju.edu.cn).

Abstract: In this paper, based on the gray value change of reflected light image of porous silicon (PSi) Bragg mirror, a fast and simple biological detection method is proposed. In this method, CdSe/ZnS quantum dots (QDs) are used as markers for refractive index amplification, and digital image method is used for detection. The detection light has the same wavelength as the lowest reflectivity of the edge of the Bragg mirror, and the reflected light radiated on the surface of the Bragg mirror is received by the detector. The theoretical simulation results show that the intensity of the reflected light increases with the increase of the refractive index caused by the biological reaction. According to the experimental results, the average gray value variation increases with the increase of the target DNA concentration and becomes a linear relationship in a certain range. Based on this method, the DNA detection limit is 20.74 pM. The method is low-cost, has a short detection time and can be used in the detection of biosensor microarray.

Index Terms: Porous silicon Bragg mirror, quantum dots, digital image, average gray value.

1. Introduction

As a nanostructured material, porous silicon has many advantages, such as large specific surface area, good biological activity and biocompatibility [1]–[3]. Electrochemical corrosion and photolithography can be used to fabricate optical devices to enhance and amplify optical signals [4], [5]. Therefore, these methods are widely used in optical biosensors [6]–[8]. At present, the main reported PSi optical biosensors are a Bragg mirror structure sensor [9], [10], a microcavity structure sensor [11], [12], and a surface grating structure sensor [13], [14]. Among them, the Bragg mirror structure is widely used. Bomin Cho *et al.* prepared distributed Bragg mirrors (DBR) via electrochemical corrosion and studied the optical properties and surface derivatization of DBR PSi and modified protein A within the DBR PSi. The biological reaction caused changes of the refractive index and detected human immunoglobulin (IgG) via the changes of the reflection spectrum [15].

There are two types of PSi optical biosensors [16], [17]. The first is a biosensor based on the detection of a change in the refractive index. The change of refractive index is reflected by

detecting the movement of reflection or Fourier change spectrum to reflect the change of the refractive index or to measure the change of the laser incident angle. Qiao Hong *et al.* proposed a label free PSi optical biosensor for the detection of protease activity. The sensing mechanism is that the effective refractive index of porous silicon is reduced and the reflection spectrum is blue shifted due to the digestion of the gelatin attached to the pores of PSi. It successfully monitors the release of Matrix Metalloproteinases (MMP) in cultured small cell groups, and provides a high-sensitivity detection method the resonant optical mode of matter molecules [18]. N. H. Maniya and co-workers prepared a label free mesoporous porous silicon optical biosensor for the detection of heat shock protein 70 (HSP70). Through the chemical methods of 3-aminopropyltriethoxysilane (APTES) and glutaraldehyde (GI), the anti-HSP70 antibody was successfully immobilized on the PSi, and the specific binding with HSP70 antigen occurred. The reflection spectrum and Fourier transform spectrum showed red shift, and the detection limit was 1290 $\pm$ 160 ng/ml. [19]. The second category is based on fluorescent change detection biosensors for biological detection of changes in fluorescence intensity produced by markers before and after biological reactions. V. Myndrul *et al.* Used a photoluminescence (PL) immunosensor based on PSi to detect ochratoxin A (OTA) at low concentrations. The interaction between anti OTA antibody modified PSi and OTA led to photoluminescence quenching. The PL intensity decreased with the increase of OTA concentration,the detection limit of 4.4 pg/ml was obtained[20]. An optical biosensor platform using PSi microcavity as luminescence enhancement was proposed by S. N. Jenie for the detection of L-lactate dehydrogenase (LDH). The fluorescence signal of LDH was 10 and 5 times higher than that of single-layer microcavity and detuning microcavity. The detection limit of LDH was 0.08 U/ml and the linear response was 0.16–6.5 u/ml [21].

In recent years, digital image method has been used in the detection of biomolecules by PSi biosensors. Chuanxi Li *et al.* prepared microarray chips based on PSi and obtained the reflected light image of the array element with a microcavity structure using digital imaging equipment. Furthermore, they calculated the average gray value of the image and then expressed the refractive index change by the change of gray value and detected each array element 10^{-4} refractive index variation [22]. Hanyue Wei *et al.* used the digital image method to detect DNA, they fixed the target DNA on the prepared PSi holes with a Bragg structure and hybridized it with the probe DNA coupled with the semiconductor colloidal CdSe/ZnS QDs. The fluorescence images of sensors with different concentrations were obtained by the digital imaging device. Target DNA was detected through the relationship between the change of the average gray value of the image and the concentration of the target DNA, and the detection limit of DNA was 88 pM [23].

In this paper, the method for detecting PSi optical biosensor based on refractive index changes is combined with a digital image method, and the variation characteristics of reflected light at the forbidden edge of the Bragg mirror are studied for the first time. The reflected light images before and after biological reaction are obtained by digital microscope, and the average gray value variation detects the refractive index change caused by biomolecular reaction, thus detecting the detection limit of DNA. This method is fast, efficient, operable and sensitive, the method is a good, new method for biological detection.

2. Detection Principle

The PSi of the Bragg mirror is a one dimensional photonic crystal composed of a high refractive index layer (low porosity) and a low refractive index layer (high porosity) that alternate periodically. The corresponding centre wavelength in the band gap width range has high reflectivity. The following relationship is satisfied:

$$m\lambda_{Bragg} = 2(n_L d_L + n_H d_H) \tag{1}$$

where m is an integer, $m\lambda_{Bragg}$ is the centre wavelength of the Bragg mirror, n_H and n_L are the two symmetrical high refractive index (low porosity) layers of the Bragg mirror and low refractive index (high porosity) layer, respectively, and d_L and d_H are the optical thickness of the high and low refractive index layer of the Bragg mirror. Fig. 1 shows the structural schematic of the Bragg mirror.

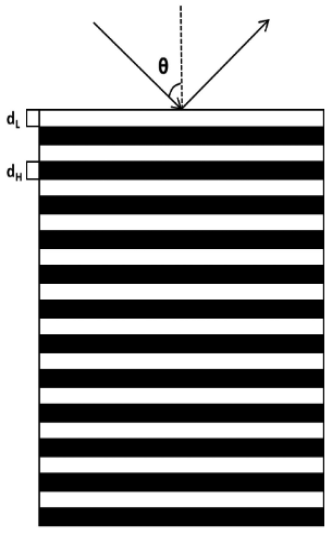

Fig. 1. Schematic diagram of the structure of the Bragg mirror.

According to the PSi Bragg formula, using the transfer matrix theory to simulate the Bragg reflection spectrum, the designed PSi Bragg mirror have 24 layers. The PSi centre wavelength of the Bragg mirror is 553 nm, and the wavelength of the lowest reflectivity position at the end edge of the band gap is 633 nm. The high refractive index and the low refractive index of the Bragg mirror are 1.41 and 1.10 respectively, the thickness of the high refractive index layer is 98 nm, and the thickness of the low refractive index layer is 126 nm. The relationship between porosity and effective refractive index of PSi can be obtained from theoretical calculation and practical measurement.

According to Bruggeman's theory [24], the effective refractive index of PSi can be obtained from formula (2) before adding any substance.

$$(1-\rho)\frac{{n_{si}}^2-{n_{eff}}^2}{{n_{si}}^2+{n_{eff}}^2}+\rho\frac{{n_{air}}^2-{n_{eff}}^2}{{n_{si}}^2+2{n_{eff}}^2}=0 \tag{2}$$

Where ρ is the porosity of PSi, n_{Si} is the refractive index of silicon, n_{eff} is the effective refractive index of PSi, and n_{air} is the refractive index of air.

According to the above formula (2), n_{eff} decreases with the increase of ρ.

The refractive index, extinction coefficient and thickness of PSi samples with different porosity are measured by ellipsometry, which are in good agreement with the theoretical calculation results.

Suppose the wavelength of the detected light is 633 nm, there is incident light on the end edge of the band gap of the PSi Bragg mirror, so the reflected light intensity is minimized and the gray value is minimized, which is recorded as G_1. When the target DNA with different concentrations are coupled with QDs, they hybridize with probe DNA, the effective refractive index of PSi devices changes accordingly and the reflection spectrum of the PSi Bragg mirror device redshifts. The reflectivity of the original forbidden band edge is the lowest at 633 nm, and the reflectivity at 633 increases slightly due to the red shift of the reflection spectrum, as shown in Fig. 2, in the figure, curves b, c, and d are the reflection spectra of theoretical simulation Bragg mirror with effective refractive index increased by 0.005, 0.01, and 0.02, respectively. At this time, the reflected light of the Bragg mirror after hybridization reaction was obtained by deflecting the same angle, and the digital microscope was used to image it, and the corresponding average gray value G_2 was calculated. Therefore, we can obtain the change amount of the average grayscale value of the Bragg mirror before and after the biological reaction ($\triangle G = G_2$ - G_1), and get the relationship with the concentration of the target DNA molecule, so as to get the detection limit of the target DNA.

When specific organism binding occurs inside the PSi, the effective refractive index of the PSi changes. The internal structure of the PSi biosensor is different, so the sensitivity to its effective

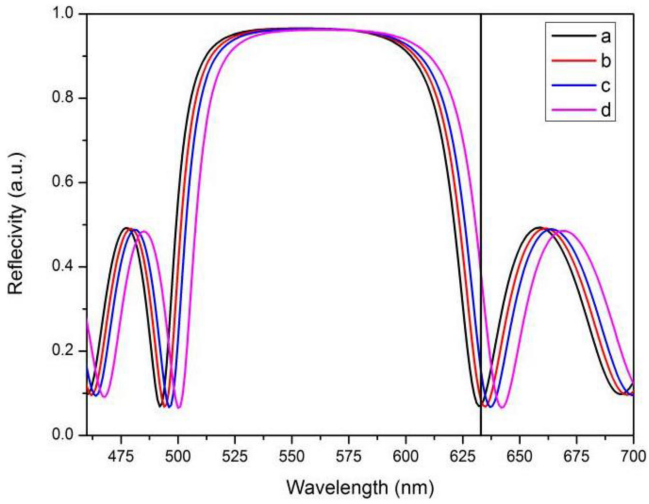

Fig. 2. Reflection spectra of the PSi Bragg mirror after increasing the effective refractive index by 0.005, 0.01, and 0.02.

refractive index changes are also different. At present, the structure of PSi microcavities is often used in the optical biosensor based on detection of the refractive index change. The structure consists of two Bragg mirrors with the same period and a central defect layer. The defect layer can produce a defect peak, which has high transmittance, half height and narrow width optical characteristics [25].

For further analysis of the sensitivity of the internal structure of the PSi biosensor to the refractive index change of the sensor, this paper compares the PSi microcavity with the PSi Bragg mirror. It is assumed that there are 25 layers in the microcavity, that the refractive indexes of the high and low refractive indexes are $n_H = 1.41$ and $n_L = 1.1$, respectively, and the refractive index of defect layer is $n_C = 1.1$. The corresponding optical thicknesses are $d_H = 98$ nm, $d_L = 126$ nm, and $d_C = 251$ nm, respectively. In an ideal state, a Bragg mirror with defect state is used as an optical biosensor. When the refractive index of the device increases, the surface reflectance spectrum of the device will redshift. By measuring the change of the wavelength of the defect state, the change of the refractive index can be indirectly measured. The theoretical analysis results show that the detection sensitivity of ideal Bragg mirror is slightly lower than that of Bragg mirror with defect state. However, in practice, due to the dispersion and absorption characteristics of the fabricated PSi photonic devices and the fluctuation of the dielectric surface, the optical properties of the PSi microcavity are greatly affected [26]. Compared with the theoretical curve of the ideal device, the half width of the defect state increases and the reflectivity increases, the quality factor is greatly reduced. On the contrary, as an optical biosensor, the optical properties at the edge of the band gap are not affected by the PSi Bragg mirror, the detection sensitivity of refractive index change is higher than that of PSi microcavity.

3. Experiments

3.1 Preparation of PSi Bragg Mirror

Using p boron doped monocrystalline silicon (crystal direction $<100>$, electrical resistivity 0.03–0.06 Ω·cm, thickness 400 $\pm$ 10 μm), a PSi Bragg mirror was prepared by anodic electrochemical corrosion. The silicon wafers were cut into small squares of 2 cm $\times$ 2 cm before the experiment. After that, acetone, anhydrous ethanol and deionized water are used for repeated cleaning, and the ultrasonic cleaning machine is used for 15min to ensure that the impurities such as grease and dust on the surface of silicon wafer are removed, and the influence of impurities on the corrosion process of PSi Bragg mirror is minimized. The electrolyte was made up of hydrofluoric acid and

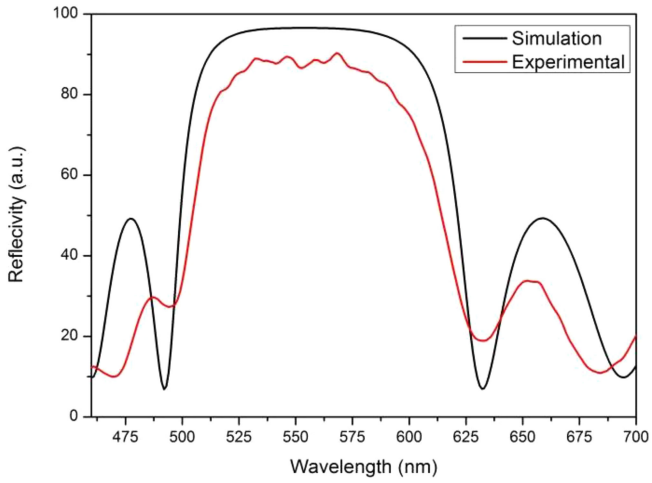

Fig. 3. Comparison of experimental and theoretical reflection spectrum of PSi Bragg mirror.

99% anhydrous ethanol with a volume ratio of 1:1, The corrosion solution was poured into the etching tank of the fixed silicon wafer. The current density in the corrosion process is controlled by Labview procedures (National Instruments Corporation, United States), the high and low current alternately constitute the PSi Bragg mirror structure. The current density of high refractive index layer and low index layer is set to 40 mA/cm^2 and 90 mA/cm^2, respectively. During the corrosion process, the interval of each layer of PSi was 3s to ensure enough fluoride ions were present and that corrosion uniformity existed. The silicon wafer was removed after corrosion, washed repeatedly with deionized water and dried in a nitrogen environment. In order to prepare five PSi Bragg mirrors with the same parameters to analyze the repeatability and stability of the performance of PSi Bragg mirror biosensor, five PSi Bragg mirrors were fabricated under the same anodic electrochemical corrosion conditions. The experimentally prepared PSi Bragg mirror devices were detected using a spectrometer with a resolution of 0.1 nm (Hitachi U-4100, purchased from Hitachi, Japan) and compared with the reflectance spectra calculated by the transfer matrix method theory. Fig. 3 shows a comparison of the reflection spectrum. It can be seen from the Fig. 3 that the center wavelength of the PSi Bragg mirror sample is 553 nm, the reflectivity is the highest, and the wavelength at the edge of the end of the forbidden band is 633 nm, and the reflectivity is the lowest. There is little difference between the reflectance spectra of the PSi Bragg mirror simulated by theory and those prepared by experiment, and they are basically consistent, so the PSi Bragg mirror sample is successfully prepared.

SEM image of PSi surface is shown in Fig. 4, and the pore size is about 20–30 nm, the length of a base pair is about 0.34 nm, the DNA molecules we used has 16 base pairs with a length of about 6 nm. The pore size of PSi ensures that the QDs modified 16 base pairs DNA molecules can enter smoothly and complete the biological detection. Fig. 5 shows a cross section of the newly prepared PSi Bragg mirror photographed by a scanning electron microscope.

3.2 Functionalization of PSi Bragg Mirror

The existence of the Si-H bond on the surface of new PSi makes it extremely easy to oxidize in air, so we need to oxidize the sample to determine the optical properties of the stable sample. The sample was soaked in a 30% hydrogen peroxide solution, and then the sample was placed in a 60 °C environment for oxidation for 3 h, which caused the surface to form a SiO_2 layer, and the sample was removed and rinsed with deionized water and anhydrous ethanol then placed atroom temperature to cool. The oxidized sample was immersed in 5% 3-aminopropyltriethoxysilane for 1 h to form an amino group and was then removed and rinsed with deionized water and ethanol.

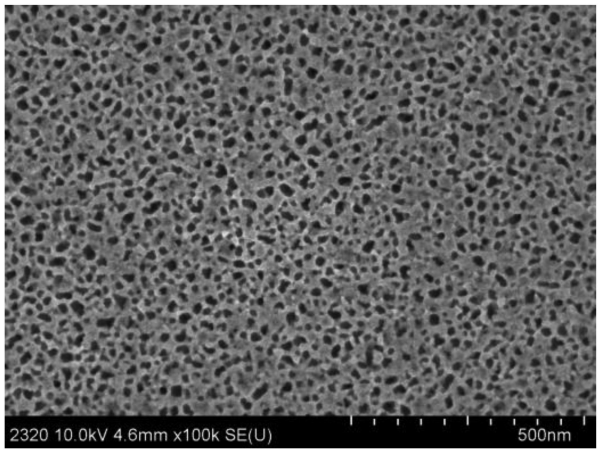

Fig. 4. SEM image of PSi Bragg mirror surface.

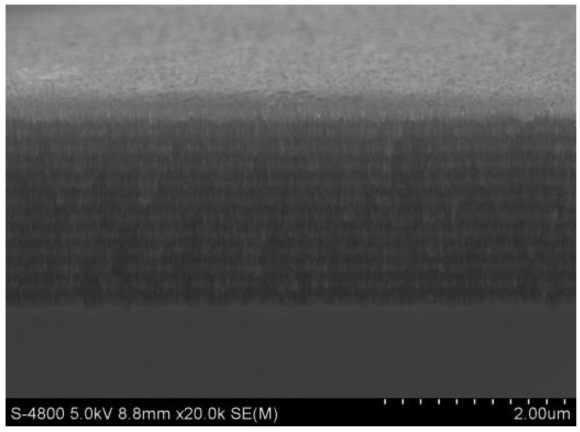

Fig. 5. SEM image of PSi Bragg mirror cross section.

The sample was placed in a vacuum dryer for 10 min at 100 °C after drying at room temperature for 1 h. The siliconized PSi sample was immersed in an aqueous solution of 2.5% glutaraldehyde for 1 h and rinsed with phosphate buffer (PBS) and deionized water to remove excess glutaraldehyde. Fig. 6 shows the contrast of the functionalized reflection spectrum of the PSi Bragg mirror. The change of the reflection spectrum in the figure indicates that each step of the functionalization is successful.

3.3 The Probe DNA Is Fixed to PSi Bragg Mirror

DNA was purchased from Ying Jie Leading (Shanghai) Trading Co., Ltd.

Probe DNA: 5'-CAACGTTGCAGTGTAC-3'-NH2

Target DNA: 5'-GTTGCAACGTCACATG-3'-NH2

The probe DNA with a concentration of 50 μL and 10 μM was dropped onto the surface of the Bragg mirror using a micropipetre. The Bragg mirror was placed in a 37 °C incubator for 2 h. After removal, it was repeatedly rinsed with a large amount of PBS and deionized water, and dried at room temperature. The dried silicon wafers were immersed in 3M ethanolamine hydrochloride and placed in 37 °C incubator for 1 h. After being removed, the silicon wafer was repeatedly washed with lots of PBS and deionized water to ensure that DNA molecules fully entered the hole. As shown in Fig. 7, when the probe DNA is fixed in the hole of PSi Bragg mirror, the reflection spectrum is

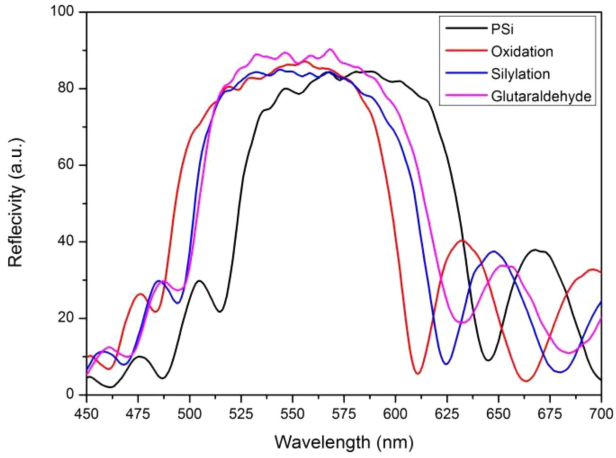

Fig. 6. Comparison of the spectra of the PSi Bragg mirror after oxidation, silylation and glutaraldehyde treatment.

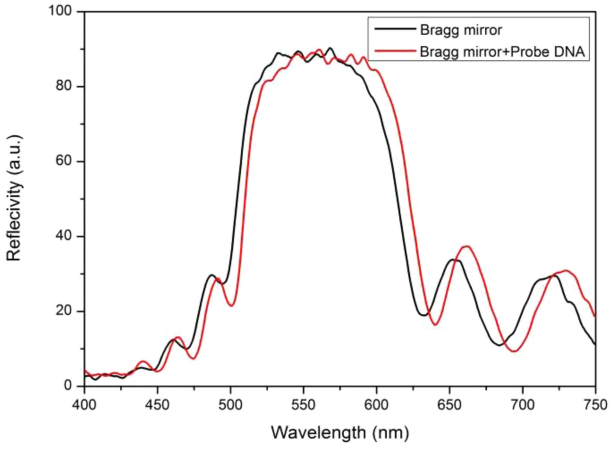

Fig. 7. Comparison of the reflection spectra of the probe DNA fixed on the pore wall of the PSi Bragg mirror.

red shifted, proving that the probe DNA probe DNA was successfully immobilized in the hole of the PSi Bragg mirror.

3.4 Coupling of Quantum Dots With the Target DNA

The water-soluble CdSe/ZnS quantum dots used in this paper were purchased from Wuhan Jiayuan Quantum Dot Co. Ltd, the particle size was 6 nm, and the fluorescence peak was at 624 nm. Fig. 8(a) shows the high-power transmission electron microscope image of QDs. A 50 μL, 8 μM QDs was dripped into a 1.5 mL microcentrifuge tube with 340 uL PBS, after stirring for 5 min, 30 μL, 0.01 M EDC and 30 μL 0.01 M sulfo-NHS were added for QDs activation and oscillatory reaction for 10 min. The final concentration of QDs was 1 μM. Then 30 μL cDNA of the required concentration is added and shaken by the light for 10 h to ensure sufficient linkage between QDs and cDNA. After removal, the cDNA is centrifuged at 10000 r/min for 15 min. A pipette is used to drop QDs modified cDNA onto the PSi Bragg mirror device with the probe DNA fixed. The device is placed in a 37 °C incubator for 2 h, and then wash repeatedly with PBS and deionized water after removal, so as to remove the QDs modified by QDs that are not connected successfully and the QDs modified cDNA that did not enter the hole to undergo hybridization reaction. The fluorescence spectra of QDs and QDs-DNA are determined by Hitachi Model F-4600 FL Spectrophotometer.

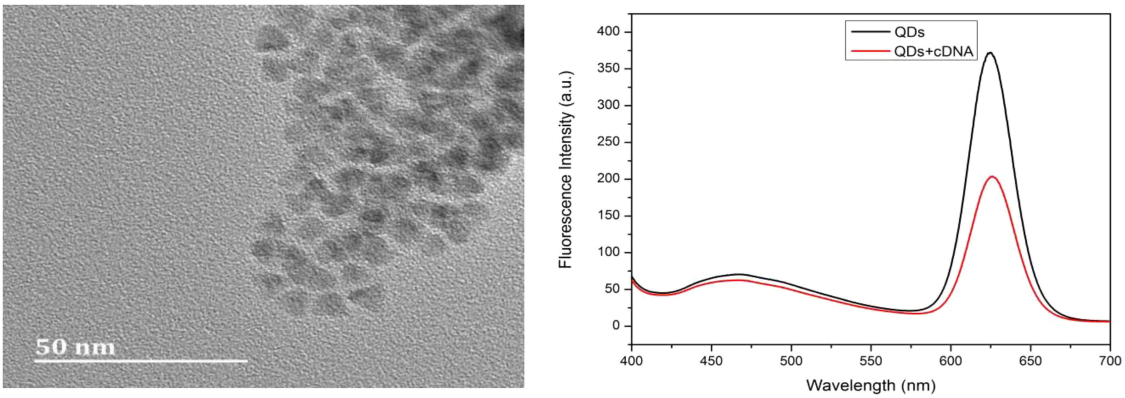

Fig. 8. (a) TEM image of QDs. (b) Fluorescence spectra before and after QDs and target DNA connection.

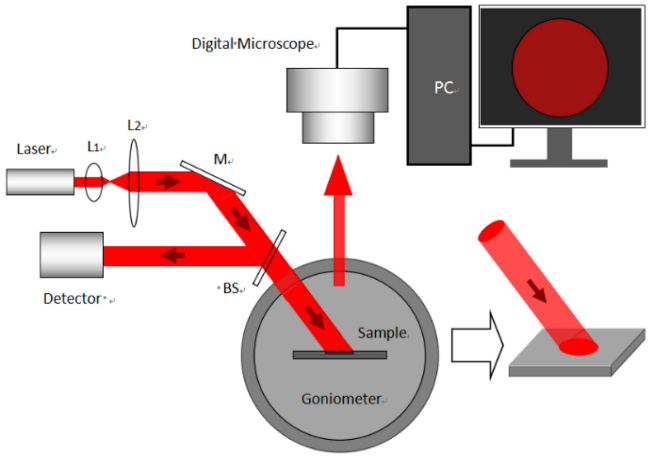

Fig. 9. Schematic diagram of the experimental device for the detection of biomolecule by digital image method.

The voltage is set to 400 v, and the slit width is 2.5 nm. When QDs was coupled with 10 μM target DNA, the fluorescence emission peak was red shifted from 624 nm to 626 nm by fluorescence spectrum detection, as shown in Fig. 8(b), indicating that QDs was successfully coupled with DNA.

3.5 Detection of the PSi Bragg Mirror by the Digital Image Method

A diagram of the experimental setup for this experiment is shown in Fig. 9. The light source is a He-Ne laser ($\lambda = 633$ nm, 1.8 mW), two lenses L_1 and L_2 form a collimated beam system. After beam expansion, part of the light reflected by the beam splitter BS is detected by detector D, which is used to correct the influence of the unstable laser power and other factors. A portion of the transmitted light hits the surface of the PSi sample placed in the centre of the goniometer G. The sample can rotate with the goniometer and reflect the incident light into the digital microscope, and image on a computer. In this optical path, the He-Ne laser, lens $L_1$and lens L_2 are in the same straight line, which reduces the loss of incident light, and the detection process is simple.

In order to facilitate the reflection of light image gray analysis, we select an area with relatively uniform gray level in the image to calculate the average gray level. The selected area is a circular area with a diameter of about two thirds of the diameter of the reflected light image (the area surrounded by the green line in Fig. 10). The center of the selected area coincides with the center

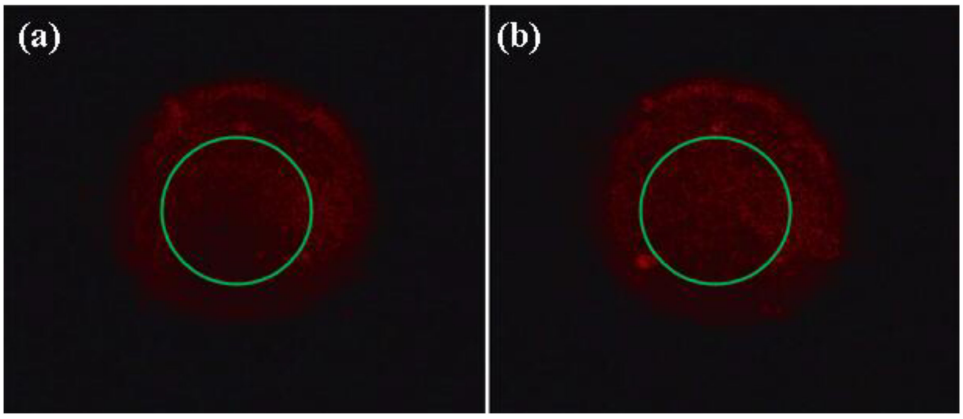

Fig. 10. Reflected light image of PSi Bragg mirror sensor. (a) No target molecules were added to the PSi, (b) The target DNA molecules with a concentration of 0.1 nM were added into the PSi, and the unreacted target molecules were washed out after the biological reaction.

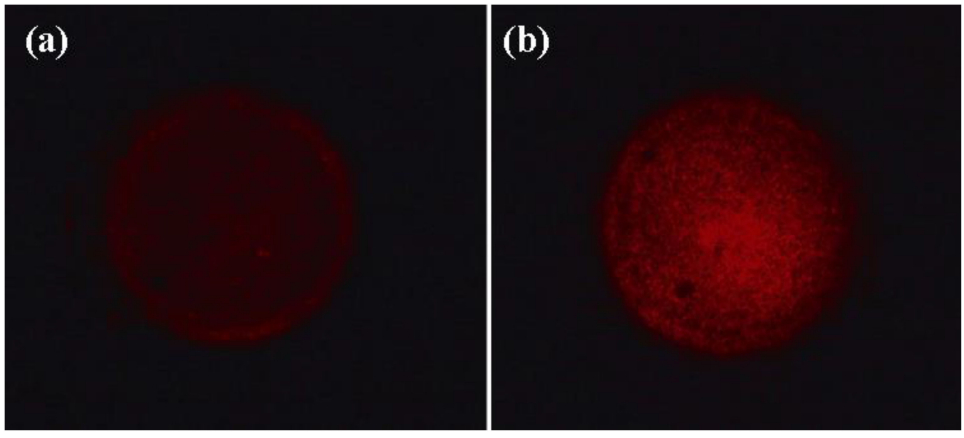

Fig. 11. Reflected light image of PSi Bragg mirror sensor. (a) No target molecules were added to the PSi, (b) The target DNA molecules with a concentration of 2 nM were added into the PSi, and the unreacted target molecules were washed out after the biological reaction.

of the reflected light image. The same area is selected as the area for the average gray value calculation of the reflected light images of the PSi Bragg mirror with different concentrations.

4. Results and Discussion

Since the PSi Bragg mirror is functionalized, its reflection spectrum will redshift and the incident angle of the incident light will be adjusted so that the detection light of 633 nm will incident on the surface of the Bragg mirror at an angle of 108°, so that the reflected light intensity is the minimum and the reflected light is the darkest. The digital microscope is used to receive the reflected light image of Bragg mirror, and the corresponding average gray value is calculated. Then, the target DNA with the concentration of 0.1 nM, 0.5 nM, 1 nM, 2 nM, 3 nM and 5 nM was hybridized with the probe DNA. The probe light at 633 nm will incident on the Bragg mirror sample surface at the same angle. The reflected light image of the functionalized PSi Bragg mirror is shown in Fig. 10(a), and the reflected light image of the target DNA added with 0.1 nM concentration is shown in Fig. 10(b). Fig. 11 shows the reflected light image of the target DNA before and after the biological reaction with the concentration of 2 nM. Some of the bright spots (Fig. 10b) and the dark spots (Fig. 11b)

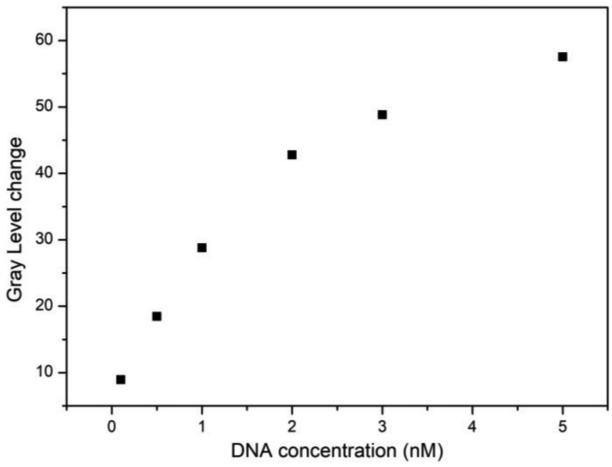

Fig. 12. Trend chart of the change of average gray value of target DNA at six concentrations.

in the reflected light image are due to the poor beam quality of the laser used. Finally, a digital microscope is used to obtain the reflected light image on the surface of the Bragg mirror after the biological reaction of six concentrations of target DNA coupled with QDs and probe DNA, and the average gray value of the area surrounded by green lines in the reflected light image is calculated.

The incident light deflects to the surface of the functionalized Bragg mirror at a certain angle, so the reflected light intensity is minimized, and its average gray value is calculated. The probe DNA is fixed on the inner wall of the hole of PSi Bragg mirror, and hybridized with the target DNA successfully coupled with quantum dots in the hole of PSi. After the incident light deflects at the same angle, the reflected light image of PSi Bragg mirror is obtained, and the corresponding average gray value is calculated. It is concluded that before and after the hybridization reaction, the values of $\triangle$G are 8.93, 18.47, 28.78, 42.78, 48.83 and 57.56. Fig. 12 shows the trend chart of the change of average gray value of target DNA at six concentrations, it can be seen from the figure that with the increasing of target DNA concentration in the PSi Bragg mirror, the change of average gray value also increases. When the DNA molecular concentration is between 0.1–5 nM, the change of average gray value increases with the increase of DNA molecular concentration, almost in a linear relationship.

In order to calculate the detection limit of the sensor, DNA molecules with concentration of 0.1 nM, 0.5 nM, 1 nM and 2 nM were selected to measure the corresponding average gray value variation. Fig. 13 shows the relationship between the change of average gray value and DNA molecules of four concentrations. It can be seen from the figure that there is a good linear relationship between the two. The linear correlation coefficient is 0.98 and the linear equation is: $Y = 18.41 \times + 7.57$.

Due to the changes in the PSi surface, there will be accidental errors during the experiment, which will affect the detection accuracy. The experimental results are calculated by the 3σ rule, where 3σ is the minimum gray value that can be resolved and σ is the standard deviation of the average gray level of the same sample before the biological reaction measured 10 consecutive times. In our experiments, the measurement value of σ is 0.13, and the detection limit is about 20.74 pM based on the minimum gray resolution value.

In the above experiment, the probe DNA was first immobilized in the hole of PSi Bragg mirror, and then hybridized with different concentrations of target DNA successfully coupled with QDs. The reflected light images before and after hybridization reaction were recorded by digital microscope, and the corresponding average gray value changes were calculated, so as to obtain the relationship between the average gray value changes and different concentrations of DNA molecules. Another method is to fix the target DNA in the hole of the PSi Bragg mirror, and then hybridize with the probe DNA which is successfully coupled with QDs, the reflected light image of the PSi Bragg

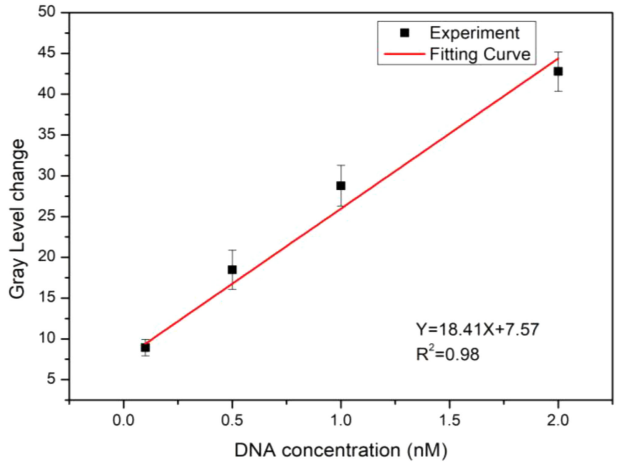

Fig. 13. The linear relationship between DNA concentration and change in mean gray value.

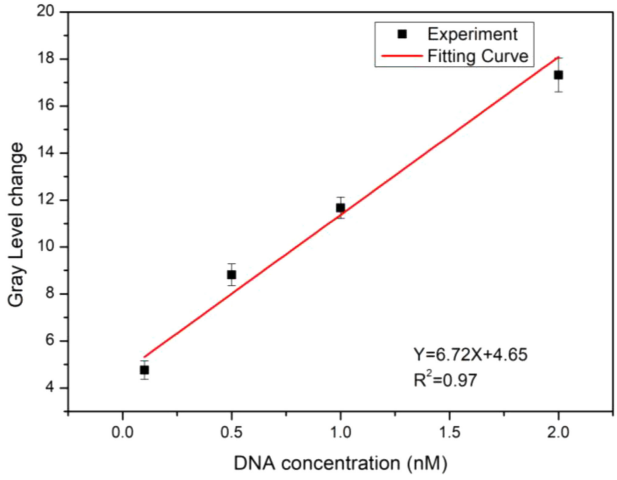

Fig. 14. The linear fitting of DNA concentration and variation of mean gray value.

mirror before and after the hybridization reaction is obtained, and the corresponding average gray value is calculated. The relationship between the average gray value change and the concentration of target DNA molecule is obtained, and finally the detection limit of DNA molecule is obtained. To better compare the two methods, using the same probe DNA molecule, QDs and target DNA molecule. The experimental results obtained by this method can be used to obtain the relationship between the change in the average gray value of the light reflected by the PSi Bragg mirror and the increase in the concentration of DNA molecules from 0.1 nM to 2 nM, as shown in Fig. 14. As can be seen from Fig. 14, the average gray value changes with the increase of the target DNA molecular concentration, and has a good linear relationship. The experiments result shows that the detection limit obtained by this method is 42.42 pM, the linear correlation coefficient is 0.97 and the linear equation is: $Y = 6.72 \times + 4.65$.

The repeatability and stability of sensor performance play a key role in accurate target detection [27]. Under the same preparation conditions, five identical PSi Bragg mirror biosensors were fabricated on monocrystalline silicon, the DNA molecules of 5 nM were detected by digital image method, which were used to detect the performance repeatability of PSi sensors. The relative standard deviation of the detection results of the five PSi sensors was 4.65%. Five identical PSi Bragg mirror biosensors were prepared and tested every five days to detect the stability of the

sensors. Using the digital image method to detect the target DNA molecules with the concentration of 5 nM, the detection results are obtained and the relative standard deviation is 5.78%. It can be seen from the experimental results that the PSi sensor has high reproducibility and stability in DNA molecular detection.

Compared with other biological detection methods, the biological detection method proposed in this paper has the following four advantages. The first advantage is that the detection method proposed by us has a lower detection limit. The detection limits of three kinds of PSi optical biosensor methods for DNA detection based on refractive index change are as follows:the detection limit of label -free and reflectance spectroscopy for DNA detection was 43.9 nM [28], the detection limit of label-free and angle spectrum method for DNA detection was 87 nM [29], using CdSe/ZnS QDs marking target DNA molecules, administered implementation refractive index amplification, detection of DNA detection limit of 36 pM [30]. The detection limit of our proposed detection method is 20.74 pM. The second advantage of this method is its low detection cost. For the PSi biosensors using reflection spectroscopy and fluorescence spectroscopy for biological detection, the spectral equipment is expensive. However, the detection method proposed in this paper does not require spectral equipment, only digital microscope and general optical devices are needed. The third advantage is the short detection time. Spectral instrument calibration and sample wavelength scanning are required in both reflectance spectrum detection and fluorescence spectrum detection. For example, it takes 38 seconds to scan a sample using an UV-visible spectrophotometer (Hitachi U-4100, Japan) and a few minutes to scan a sample using a fluorescence spectrometer (Hitachi F-4600, Japan) [31]. The detection method used in this paper first uses a digital microscope to obtain the reflected light image on the surface of the PSi Bragg mirror, then the average gray value of the image is calculated by the corresponding algorithm. It takes several seconds to complete the process. The fourth advantage is the high bioassay throughput. For the detection of PSi optical biosensor microarray, spectroscopic detection requires the help of positioning equipment to detect each unit on the array one by one, and gray value calculation method based on digital image on the surface of the array average gray value calculation can parallel detecting the change of the average gray value of each unit [32], so as to achieve different concentrations of biological set in a microarray devices, conduct biological detection [33], we put forward the detection method can realize the PSi optical biosensor microarray fast parallel detection.

5. Conclusion

A new method for the detection of biomolecules by PSi Bragg mirror biosensor is presented, which is based on CdSe/ZnS water-soluble QDs successfully labeled the target DNA as the marker to amplify the refractive index of the reactants. Digital imaging equipment is used to capture the reflected light images before and after hybridization of probe DNA and target DNA coupled with QDs, and the variation of its average gray value was calculated. As a result, the average gray value before and after biological reaction changes linearly with the change of the target DNA concentration, and the detection limit is 20.74 pM. This method can realize fast, highly efficient, low cost and high sensitivity biological detection. Furthermore, the process can be applied for biological parallel monitoring of PSi arrays.

References

[1] O. Meskini, A. Abdelghani, A. Tlili, R. Mgaieth, N. Jaffrezic-Renault, and C. Martelet, “Porous silicon as functionalized material for immunosensor application,” *Talanta*, vol. 71, pp. 1430–1433, 2007.
[2] K. Urmann, S. Arshavsky-Graham, J. G. Walter, T. Scheper, and E. Segal, “Whole-cell detection of live lactobacillus acidophilus on aptamer-decorated porous silicon biosensors,” *Analyst*, vol. 141, pp. 5432–5440, 2016.
[3] S. Arshavsky-Graham, N. Massad-Ivanir, E. Segal, and S. Weiss, “Porous silicon-based photonic biosensors: Current status and emerging applications,” *Anal. Chem.*, vol. 91, pp. 441–467, 2019.
[4] J. D. Ryck man, M. Liscidini, J. E. Sipe, and S. M. Weiss, “Porous silicon structures for low-cost diffraction-based biosensing,” *Appl. Phys. Lett.*, vol. 96, no. 17, 2010, Art. no. 171103.

[5] V. H. Pham *et al.*, "Progress in the research and development of photonic structure devices," *Adv. Natural Sci.: Nanoscience Nanotechnol.*, vol. 7, 2016 doi: 10.1088/2043-6262/7/1/015003.
[6] K. M. Victor S.-Y. Lin, K.-P. S. Dancil, M. J. Sailor, and M. Reza Ghadiri, "A porous silicon-based optical interferometric biosensor," *Science*, vol. 278, no. 5339, pp. 840–843, 1997.
[7] H. J. Kim, Y. Y. Kim, K. W. Lee, and S. H. Park, "A distributed bragg reflector porous silicon layer for optical interferometric sensing of organic vapor," *Sensors Actuators B: Chem.*, vol. 155, pp. 673–678, 2011.
[8] X. Wei, *et al.*, "Grating couplers on porous silicon planar waveguides for sensing applications," *J. Appl. Phys.*, vol. 104, no. 12, 2008, Art. no. 123113.
[9] D. Dovzhenko, E. Osipov, I. Martynov, P. Linkov, and A. Chistyakov, "Enhancement of spontaneous emission from CdSe/CdS/ZnS quantum dots at the edge of the photonic band gap in a porous silicon Bragg mirror," *Phys. Procedia*, vol. 73, pp. 126–130, 2015.
[10] P. A. Snow, E. K. Squire, P. S. J. Russell, and L. T. Canham, "Vapor sensing using the optical properties of porous silicon bragg mirrors," *J. Appl. Phys.*, vol. 86, pp. 1781–1784, 1999.
[11] F. S. H. Krismastuti, S. Pace, and N. H. Voelcker, "Porous silicon resonant microcavity biosensor for matrix metalloproteinase detection," *Adv. Funct. Materials*, vol. 24, pp. 3639–3650, 2014.
[12] V. M. Z. G. a. L. Pavesi, "Porous silicon microcavities as optical and eletrical chemical sensors," *Phys. Lett.*, vol. 182, pp. 479–484, 2000.
[13] S. Sahu, J. Ali, P. P. Yupapin, and G. Singh, "Porous silicon based Bragg-grating resonator for refractive index biosensor," *Photonic Sensors*, vol. 8, pp. 248–254, 2018.
[14] G. A. Rodriguez, J. D. Ryckman, Y. Jiao, and S. M. Weiss, "A size selective porous silicon grating-coupled bloch surface and sub-surface wave biosensor," *Biosensors Bioelectron.*, vol. 53, pp. 486–493, 2014.
[15] B. Cho, B. Y. Lee, H. C. Kim, H. G. Woo, and H. Sohn, "Fabrication of human IgG sensors based on porous silicon interferometer containing bragg structures," *J. Nanosci. Nanotechnol.*, vol. 12, pp. 4159–4162, 2012.
[16] I. Rendina, I. Rea, L. Rotiroti, and L. De Stefano, "Porous silicon-based optical biosensors and biochips," *Physica E: Low-dimensional Syst. Nanostructures*, vol. 38, pp. 188–192, 2007.
[17] M. A. Anderson *et al.*, "Sensitivity of the optical properties of porous silicon layers to the refractive index of liquid in the pores," *physica status solidiv (a)*, 197, pp. 528–533, 2003.
[18] H. Qiao, B. Guan, J. J. Gooding, and P. J. Reece, "Protease detection using a porous silicon based bloch surface wave optical biosensor," *Opt. Exp.*, vol. 18, pp. 15174–151825, 2010.
[19] N. H. Maniya and D. N. Srivastava, "Fabrication of porous silicon based label-free optical biosensor for heat shock protein 70 detection," *Materials Sci. Semicond. Process.*, vol. 115, 2020, Art. no. 105126.
[20] V. Myndrul *et al.*, "Porous silicon based photoluminescence immunosensor for rapid and highly-sensitive detection of Ochratoxin A," *Biosensors Bioelectron.*, vol. 102, pp. 661–667, 2018.
[21] S. N. Jenie, B. Prieto-Simon, and N. H. Voelcker, "Development of L-lactate dehydrogenase biosensor based on porous silicon resonant microcavities as fluorescence enhancers," *Biosensors Bioelectron.*, vol. 74, pp. 637–643, 2015.
[22] C. Li, Z. Jia, P. Li, H. Wen, G. Lv, and X. Huang, "Parallel detection of refractive index changes in a porous silicon microarray based on digital images," *Sensors (Basel)*, vol. 17, no. 4, 2017, Art. no. 750.
[23] H. Wei *et al.*, "Detection using a quantum dots/porous silicon optical biosensor based on digital fluorescence images," *Sensors Actuators B: Chem.*, vol. 315, 2020, Art. no. 128108.
[24] E. V. Astrova and V. A. Tolmache, "Effective refactive index and composition of oxidized porous silicon films," *J. Materials Sci. Eng.*, vol. 69–70, pp. 142–148, Jan. 2000.
[25] S. Surdo and G. Barillaro, "Impact of fabrication and bioassay surface roughness on the performance of label-free resonant biosensors based on one-dimensional photonic crystal microcavities," *ACS Sensors*, vol. 5, no. 9, pp. 2894–2902, 2020.
[26] C. C. Li, Z. H. Jia, L. He, and X. H. Huang, "Effects of dispersion, absorption and interface fluctuation on the reflection spectra of porous silicon microcavity devices," *Optoelectron. Lett.*, vol. 15, pp. 89–92, 2019.
[27] M. Y. Emran, S. A. El-Safty, M. A. Shenashen, and T. Minowa, "A well-thought-out sensory protocol for screening of oxygen reactive species released from cancer cells," *Sensors Actuators B: Chem.*, vol. 284, pp. 456–467, 2019.
[28] H. Zhang *et al.*, "Porous silicon optical microcavity biosensor on silicon-on-insulator wafer for sensitive DNA detection," *Biosensors Bioelectron.*, vol. 44, pp. 89–94, 2013.
[29] P. Li *et al.*, "Spectrometer-free biological detection method using porous silicon microcavity devices," *Opt Exp.*, vol. 23, no. 19, pp. 24626–24633, 2015.
[30] R. Zhou, Z. Jia, X. Lv, and X. Huang, "The enhanced sensitivity of a porous silicon microcavity biosensor based on an angular spectrum using CdSe/ZnS quantum dots," *Sensors*, vol. 19, no. 22, 2019, Art. no. 1872.
[31] M. Zhang, Z. Jia, X. Lv, and X. Huang, "Biological detection based on the transmitted light image from a porous silicon microcavity," *IEEE Sensors J.*, vol. 20, no. 20, pp. 12184–12189, Oct. 2020.
[32] R. Ren, Z. Jia, J. Yang, and N. Kasabov, "Applying speckle noise suppression to refractive indices change detection in porous silicon microarrays," *Sensors (Basel)*, vol. 19, no. 13, 2019, Art. no. 2975.
[33] W. Chen, Z. Jia, P. Li, G. Lv, and X. Lv, "Refractive index change detection based on porous silicon microarray," *Appl. Phys. B*, vol. 122, 2016, Art. no. 120.